Geographical discrimination of extra-virgin olive oils from the Italian coasts by combining stable isotope data and carotenoid content within a multivariate analysis

S. Portarena [a*], C. Baldacchini [a], E. Brugnoli [a & b]

[a] Istituto di Biologia Agroambientale e Forestale, Consiglio Nazionale delle Ricerche, 05010, Porano (TR), Italy

[b] Dipartimento di Scienze del Sistema Terra e Tecnologie per l'Ambiente, Consiglio Nazionale delle Ricerche, 00185, Roma, Italy

*Corresponding author. Tel.: +39 0763 374909; fax: +39 0763 374980.

E-mail address: silvia.portarena@ibaf.cnr.it (S. Portarena)

Abstract

We have determined the isotopic composition and the carotenoid contents of 38 extra-virgin olive oils (EVOOs) from seven regions along the Italian coasts, by means of isotope ratio mass spectrometry (IRMS) and resonant Raman spectroscopy (RRS), respectively. The application of linear discriminant analysis to our overall results demonstrated the combination of isotope and carotenoid data is a promising method to discriminate EVOOs from production sites that are impacted by similar geographical and climatic parameters. In particular, this dual approach allowed correct classification of 82% EVOO samples, while separate IRMS and RRS investigations were able to discriminate only samples from Sicily and Latium, respectively.

Keywords: Olive oil, Raman spectroscopy, isotope ratio mass spectrometry, carotenoid content, chemometrics, geographical origin.

1. Introduction

Extra-Virgin Olive Oil (EVOO) is produced by physical extraction from the fruits of the *Olea europaea* tree. The geographical origin of EVOO is one of the most relevant factors that determine its quality and, thus, its commercial value, since the EVOO composition and nutraceutical values may depend on regional differences in climate, soil, agricultural practices and local cultivars. Thus, the European Union (EU) has set regulations for the protection of claims relating to geographic indications and origin designations for EVOOs (Woodcock, Downey, & O'Donnell, 2008), and products from defined high-quality oil-producing regions may use a Protected Designation of Origin (PDO) or Protected Geographical Indication (PGI) on their labels. For these reasons, food processors, retailers, enforcement agencies, and consumers require an independent mechanism to confirm that any given EVOO claiming PDO or PGI status actually complies with all relevant specifications.

The development of analytical methodologies for EVOO authentication is, thus, a challenging task, and several experimental techniques have been employed to assure olive oil traceability and authenticity. Chromatographic techniques, such as gas chromatography (Aparicio & Aparicio-Ruìz, 2000), gas chromatography mass spectrometry (Spangenberg & Ogrinc, 2001), and high performance liquid chromatography (Christopoulou, Lazaraki, Komaitis, & Kaselimis, 2004) have been employed to estimate the content of specific compounds (such as fatty acids, sterols, phenolics or hydrocarbons) as a function of olive oil geographical origin. Isotope ratios mass spectrometry (IRMS) has demonstrated that EVOOs from different production sites can be discriminated based on their stable isotopic composition (Angerosa et al., 1999; Camin et al., 2010). Nuclear magnetic resonance (Mannina, Patumi, Proietti, Bassi, & Segre, 2001), solid-phase micro-extraction gas chromatography-mass spectrometry (SPME-GC) (Young, Quinn & Trumble 2012), and spectroscopic techniques, such as near infrared (Casale, Casolino, Oliveri, & Forina, 2010), Fourier-transform infrared (Tapp, Defernez, & Kemsley, 2003) and Raman (Korifi, Le Dreau, Molinet, Artaud, & Dupuy, 2011) spectroscopies have allowed olive oil origin to be determined using fingerprinting approaches.

However, when a specific meteorological or geographical factor affects different geographical regions similarly, EVOOs may be difficult to distinguish if analysed using a technique that is sensitive to that parameter. In this case, an improved classification of food products can be achieved by combining the analytical data obtained using different techniques, within a multivariate approach (Casale, Casolino, Oliveri, & Forina, 2010; Chiavaro et al., 2011).

In particular, we have previously shown that the combination of $^{13}C/^{12}C$ and $^{18}O/^{16}O$ data, as measured by IRMS, could provide information about the geographical origin of olive oil (Portarena, Gavrichkova, Lauteri, & Brugnoli, 2014; Portarena et al., 2015). However, the water cycle has a significant impact on carbon and oxygen isotope composition in plant tissues, which is mediated by the evaporative demand of the geographical origin, stomatal conductance, and photosynthetic capacity. Thus, stable isotope analysis may fail in discriminating plant materials coming from regions where the meteorological cycle of evaporation, condensation, and precipitation is impacted by similar climate parameters, as occurring along the Italian coasts (Longinelli & Selmo, 2003).

Resonant Raman spectroscopy (RRS) is able to excite resonantly the vibrational modes of carotenoid pigment molecules, allowing a comparative quantification of carotenoid content (El-Abassy, Donfack, & Materny, 2009). This may depend on climatic parameters, such as light exposition, distance from the sea, temperature, and amount of precipitations (Issaoui et al., 2010). However, the carotenoid content can be affected also by genetic factors, mainly related to the olive variety (Giuffrida, Salvo, Salvo, La Pera, & Dugo, 2007), agronomical aspects, such as nutrient availability and fruit ripening (Baccouri et al., 2008), and processing and storage conditions (Gimeno, Castellote, Lamuela, De la Torre, & Lopez-Sabater, 2002). Since all these aspects may be specific of the olive growing region, the carotenoid content could be a good candidate as EVOO geographical tracer.

In this preliminary work, we selected EVOO samples coming from PDO production areas along the Italian coasts, which is a macro-region characterized by similar climatic and geographical factors,

and analysed isotopic composition and carotenoid content by means of IRMS and RRS, respectively. The geographical discrimination of our EVOO samples based on these two parameters is unsatisfactory if considered separately. However, by combining IRMS and RRS outputs within a multivariate statistical method, the analysis resulted in a prediction model that was able to classify correctly 82% of our EVOO samples.

Thus, the combination of isotope data and carotenoid content is a promising experimental approach to discriminate geographically EVOOs, even if their production sites are impacted by similar geographical and climatic parameters.

2. Materials and methods

2.1 Sampling sites

EVOO samples from 38 different sites located in seven different Italian regions (Apulia, Latium, Ligury, Molise, Sardinia, Siciliy, Tuscany) were collected during the 2011 harvest. Olives were harvested and milled by local farmers, and olive oil samples were then given to us by the Consorzio Olivicolo Italiano (UNAPROL). Sampling sites were selected along the Italian coasts, in a belt of 70 km, to reduce the so-called 'continental effect' (Angerosa et al., 1999), and they are shown in Fig. SM1 (see Supplementary Material).

The olive growing areas were differentiated by latitude, longitude, altitude and climatic conditions. Geo-climatic information on the sampling sites are reported in Table SM2 (see Supplementary Material). Colleagues from the Institute of Atmospheric Sciences and Climate of National Research Council (CNR-ISAC) provided temperature, total rainfall and relative humidity mean values. Latitude and longitude were taken from Google Earth (www.googleearth.com). The farmers provided data of harvest and altitude, based on their local knowledge.

2.2 Stable isotope analysis

Analyses of $^{13}C/^{12}C$ and $^{18}O/^{16}O$ isotope content ratio were performed using an isotope ratio mass spectrometer (Isoprime, GV, Cheadle, UK) connected to an elemental analyser (NA1500, Carlo Erba, Milan, Italy) and to a pyrolysis system (Euro Pyr-OH, Euro Vector Instruments & Software, Milan, Italy). Isotopic compositions were scale normalized with IAEA international standards, on two contemporaneously analysed scale anchors, and are expressed as δ notation according to the expression: $\delta = (R_s - R_{std}) / R_{std} \times 1000$, where R_s is the isotope ratio of the sample and R_{std} is the isotope ratio of the international standard. In particular NBS-22 fuel oil and IAEA-CH6 sucrose were used for scale normalization of measured $\delta^{13}C$ values to the VPDB scale; IAEA-601 and IAEA-602 were used for scale normalization of measured $\delta^{18}O$ values to the VSMOW scale.

The standard deviation of replicate measurements for each standard and sample was ± 0.1‰ for $\delta^{13}C$, and ± 0.3‰ for $\delta^{18}O$. Possible changes in analytical conditions within a run were corrected using NBS-22 fuel oil and IAEA-CH6 sucrose for $\delta^{13}C$ measurements and IAEA-601 (IAEA) and IAEA-CH6 sucrose ($\delta^{18}O$ = +36.4‰VSMOW) for $\delta^{18}O$. This latter reference was assigned since 2005 (Boschetti & Iacumin, 2005) and accepted in the European TRACE project (contract No. FP6-2003-FOOD-2-A 006942).

2.3 Raman spectroscopy analysis

Samples of selected EVOOs were dripped on to glass microscope slides and illuminated by the 514.5 nm line of an Argon laser with an excitation power of less than 5 mW on the sample. The laser was focused within the drop using a microscope equipped with a 10x objective. The scattered signal was then recorded at 180° backscattered geometry and dispersed by a single monochromator with a 1800 grooves/mm diffraction grating. The spectrometer (Super Labram, Jobin Yvon) was equipped with a liquid nitrogen cooled charge coupled device (CCD) detector with a resolution better than 5 cm^{-1}. Energy calibration was adjusted daily, by using a Si single crystal as a reference sample.

For each EVOO sample, RR spectra in the 900-1800 cm^{-1} range were acquired from four different points on the droplet. The intensity variability among spectra from the same sample was less than 5%. Each spectrum was obtained by averaging five scans of 10 s each. The weak fluorescence background was subtracted from the spectra by an automatic procedure implemented in the LabSpec5 software (Horiba Scientific, Edison, New Jersey). The four spectra representative of each sample were averaged before the statistical analysis.

2.4 Statistical treatment of data

The data were statistically evaluated using Statistica v8 (StatSoft Italia srl, Padua, Italy). First, principal component analysis (PCA) was performed using as input variables the intensities of Raman bands listed in SM3 (see Supplementary Material), properly normalized at the intensity of the peak located at 1440 cm^{-1} (Zou et al., 2009). This allowed us to study the structure of the dataset, and to detect the most discriminating coordinates (principal components, PCs).

Linear discriminant analysis (LDA) classification model was then developed using as input variables the PCs obtained by PCA, together with the carbon and oxygen isotopic values, after suitable variable standardization. Canonical variates (CVs) were obtained from LDA as the vectors minimizing the Wilks' lambda parameter, which is calculated as the sum of squares of the distances between points belonging to the same category divided by the total sum of squares. Values of Wilks' lambda approaching zero are obtained with well resolved categories, whereas overlapped categories make Wilks' lambda to approach one.

To test the predictive discrimination power and the stability of the obtained classification model, this was further cross-validated using standard approaches. In detail, 5 different sets of 7 oils (one for each region, randomly selected) were removed from the dataset. Each time, the model was calculated based on the remaining 31 cases and then validated with all 38 samples.

3. Results and discussion

3.1 Isotopic results

Stable isotope data for all the EVOO samples are plotted in Fig.1. Each sample is represented by a symbol in a bidimensional plane with $\delta^{13}C$ and $\delta^{18}O$ values as coordinates.

The range of variation in $\delta^{13}C$ was about 2.7‰, (from -30.2‰ to -27.5‰), while a wider range of 4.8‰ is found for $\delta^{18}O$ (from 21.7‰ to 26.5‰). Interestingly, the relatively high $\delta^{18}O$ and $\delta^{13}C$ values (up to 26.5‰ and -27.5‰, respectively) values (…) obtained for EVOOs from Sicily were due to the markedly hot climate characterizing the region, and to the related plant physiological response. In fact, hot and dry weather conditions may induce partial stomatal closure, with the consequent decrease in intercellular and atmospheric CO2 concentration ratio and increase in $\delta^{13}C$ and $\delta^{18}O$. However, the isotopic data ranges found in the present study were smaller than those recently observed by our laboratory on a more heterogeneous set (Portarena, Gavrichkova, Lauteri, & Brugnoli, 2014). As a result, the sample clustering is not clear, likely due to the influence of the so-called “coast effect” on climatic parameters and, hence, on the isotopic composition of plant tissues (Longinelli & Selmo, 2003).

3.2 Resonant Raman spectroscopy results

Representative RR spectra collected from the 38 EVOO samples are shown in Fig. 2. All the spectra presented the same Raman features, which are located at 965 cm^{-1}, 1004 cm^{-1}, 1081 cm^{-1}, 1155 cm^{-1}, 1270 cm^{-1}, 1301 cm^{-1}, 1440 cm^{-1}, 1522 cm^{-1}, 1655 cm^{-1}, and 1748 cm^{-1}, in agreement with previous EVOO RRS investigations (El- Abassy, Donfack, & Materny, 2009). The Raman bands are listed in SM3 (see Supplementary Material), together with the corresponding chemical groups, vibrational modes and molecules. In particular, we have attributed the bands at 965 cm^{-1} (C=C bending out-of-plane), 1081 cm^{-1} (C-C stretching), 1301 cm^{-1} (C-H twisting), 1440 cm^{-1} (C-H scissoring), and 1655 cm^{-1} (C=C stretching) to free fatty acids (FFAs) (Yang & Irudayaraj, 2001; El- Abassy, Donfack, &

177 Materny, 2009), and the band at 1748 cm^{-1} to triglycerides (C=O stretching in the ester linkage
178 between a fatty acid and the glycerol) (Weng, Weng, Tzeng, & Chen, 2003). The relative spectral
179 intensity of these bands was similar for all the spectra, indicating that the composition in terms of
180 fatty acids of our EVOO samples were similar. Contrary to this, a strong variability is observed in the
181 spectral intensity of the three main bands due to the resonant excitation of the carotenoid vibrational
182 modes, which are located at 1004 cm^{-1} (C-CH_3 bending), 1155 cm^{-1} (C-C stretching) and 1522 cm^{-1}
183 (C=C stretching) (Merlin, 1985; El- Abassy, Donfack, & Materny, 2009). This indicates that our
184 samples were highly heterogeneous in term of carotenoid content and composition. A separate
185 comment is required for the band at 1270 cm^{-1}: it is generally attributed to the C-H in-plane bending
186 of FFAs (Yang & Irudayaraj, 2001; El- Abassy, Donfack & Materny, 2009), but possibly also to the
187 coupling of the C-H in-plane bending and C-C stretching modes of carotenoids (Koyama et al., 1982;
188 Merlin, 1985; Berezin & Nechaev, 2005).
189
190 **3.3 Principal component analysis of resonant Raman data**
191 PCA was performed using as input variables the normalized intensities of selected Raman bands, and
192 9 PCs are obtained. The list of the first 5 PCs and their scores, together with eigenvalues and explained
193 variance, is shown in SM4 (see Supplementary Material). The scores for 38 EVOO samples on the
194 two-dimensional plane defined by the first two PCs are shown in Fig. 3. The percentage of variance
195 explained by PC1 and PC2 was 67% and 19%, respectively.
196 According to the variable loadings listed in SM4, the descriptors contributing most in PC1 were the
197 spectral intensities of the Raman bands at 1004 cm^{-1} and 1270 cm^{-1}. This confirms that the carotenoid
198 content is the most discriminating factor, and also suggests that the 1270 cm^{-1} band may be linked to
199 carotenoids rather than to FFAs. Differentiation on PC2 axis was explained mainly explained by the
200 intensity of the Raman bands at 1655 cm^{-1} and 1081 cm^{-1}, which are both due to FFA vibrational
201 modes. This indicates that the FFA composition of our EVOO samples was slight different. Indeed,
202 the three main FFAs of EVOO (oleic acid, palmitic acid and linoleic acid) have the same vibrational

203 structure (i.e., vibrational modes at about 1655 cm^{-1}, 1440 cm^{-1}, and 1081 cm^{-1}) but different relative
204 spectral intensities of the peaks (Gelder, Gussem, Vandenabeele, & Moens, 2007). For instance, the
205 intensity ratio between the band at 1655 cm^{-1} and that at 1440 cm^{-1} was about 0.7 in the oleic acid
206 spectrum, about 0.1 in the palmitic acid spectrum, and about 2.4 in the linoleic acid spectrum
207 Thus, PCA indicates that our EVOO samples had different total carotenoid contents (major
208 contribution, due to PC1) and different FFA compositions (minor contribution, due to PC2). Both of
209 these differences can be induced by differences in weather conditions during growth and harvesting
210 (Issaoui et al., 2010), genetic factors (Giuffrida, Salvo, Salvo, La Pera, & Dugo, 2007), agronomical
211 practices (Baccouri et al., 2008) and oil extraction system (Gimeno, Castellote, Lamuela, De la Torre,
212 & Lopez-Sabater, 2002). However, the class separation as obtained by PCA was not satisfactory: only
213 a partial separation of Latium and Tuscany samples from the rest of the data was obtained (see Fig.
214 3), which may arise from the peculiar varieties and/or agricultural and extraction practices
215 characterizing these two regions.
216
217 **3.4 LDA of combined IRMS and RRS data**
218 The results obtained by IRMS and RRS separately were combined within a LDA. CVs obtained,
219 together with Wilks' Lambda, p values and eigenvalues, are presented in Table 1. The first two CVs
220 were described mainly by the content in terms of $\delta^{18}O$ (CV1) and carotenoids (CV2, mostly dependent
221 on PC1). The bidimensional plot for CV1 and CV2 scores is shown in Fig. 4: a clearer discrimination
222 of the regional origin for our samples was obtained, with respect to individual IRMS and RRS
223 analyses. In particular: Sicily, Sardinia and Ligury EVOOs were well separated from the rest of the
224 samples; Latium, Tuscany and Molise data were clustered satisfactorily; Apulia oils are not well
225 grouped.
226 According to this description, the classification model derived by LDA (shown in Table 2) correctly
227 classified 82% of EVOO samples. In particular, correct predictions were obtained for five regions,
228 while low prediction percentages were obtained for Latium (57%) and Apulia (50%); this is probably

due to the morphological and climatic inhomogeneity of the sampling sites. To test the predictive discrimination power and the stability of the model, it was cross-validated using five different sets of EVOOs, as described in Section 2.4, and obtained the correct classification for 77±5 % of the unknown samples.

4. Conclusions

EVOOs from selected sites along the Italian coast are not well discriminated geographically based on either their carbon and oxygen isotopic composition or carotenoid content, when analysed separately. This might be due to the similarity in geo-climatic conditions for some of the locations. With the aim of enhancing differences among the oils, we explored the potential for improved geographical classification based on the combination of these parameters within a multivariate statistical approach. The proposed model resulted in the correct classification of 82% of samples. Even if this percentage is not very high (based on a small sample size), the model was stable.

The inclusion of other analyses could improve the accuracy of this prediction model. For example, based on our results, the different free fatty acids composition of EVOOs could be included using chromatographic techniques, such as gas chromatography - flame ionisation detector (GC-FID) or gas chromatography–mass spectrometry (GC-MS).

Similarly, the dependence of isotopic and lipid composition of EVOOs on genetic, agronomic and processing factors needs to be investigated in order to develop more sensitive tools for traceability.

Aknowledgement

The authors acknowledge UNAPROL for funding partially the research and for the assistance in providing contacts for the samples collection; Luciano Spaccino is duly recognised for his skilful execution of IRMS analyses. Thanks are due to Prof. Cannistraro and to the staff of the Biophysics and Nanoscience Centre of the University of Tuscia (Viterbo, Italy) for providing the Raman spectroscopy facilities and support.

Appendix A. Supplementary data

Supplementary data associated with this article can be found, in the online version, at http://dx.doi.org/10.1016/j.foodchem.2016.07.135**.**

Figure captions

Figure 1. $\delta^{13}C$ and $\delta^{18}O$ values of 38 EVOO samples from seven different Italian regions, collected from sites along the Italian coast. Samples from the same geographical region are represented by the same symbol, according to the legend.

Figure 2: Representative RR spectra (one per each sampling site) with indicated the major Raman bands. The spectra are shown after background subtraction and intensity normalization at the 1440 cm^{-1} peak. The spectra showing the highest and the lowest carotenoid-related band intensities (which are obtained from a Latium and a Ligury oil, respectively) are drawn as black curves. The other spectra are shown in grey, to demonstrate the variability of the RRS data.

Figure 3. Scatterplot of the scores of 38 EVOO samples on the two-dimensional plane defined by the first two PCs as calculated by PCA of the normalized intensities of selected Raman bands. Each EVOO sample is represented by a symbol, grouped by the region of origin, according to the legend.

Figure 4. Scatterplot of the scores of 38 EVOO samples on the two-dimensional plane defined by the CV1 and CV2 resulting from a LDA of combined IRMS and RRS results (as obtained by PCA), after variable standardization. Each EVOO sample is represented by a symbol, grouped by the region of origin, according to the legend.

Table 1. Structure matrix of the model from LDA, together with statistical values of Wilks' Lambda, p value and eigenvalue calculated for each CV.

	CV1	CV 2	CV 3	CV 4	CV 5
PC1std	-0.548	0.947	-0.209	-0.267	-0.044
PC2std	0.407	0.110	0.850	0.121	0.239
PC3std	-0.360	0.258	0.276	-0.055	-0.198
PC4std	0.028	0.279	-0.005	0.548	0.151
PC5std	0.733	0.172	-0.085	-0.171	0.186
PC6std	0.229	0.501	0.354	-0.401	-0.288
PC7std	0.206	0.208	0.052	0.012	0.140
PC8std	-0.206	0.111	0.501	-0.164	0.020
PC9std	0.186	0.406	-0.340	-0.832	0.182
δ^{13}Cstd	0.198	-0.196	-0.418	0.475	-0.779
δ^{18}Ostd	-1.368	0.112	-0.042	0.594	0.295
Wilks' Lambda	0.013	0.069	0.193	0.433	0.731
p value	0.000	0.013	0.121	0.496	0.845
Eigenvalue	4.304	1.794	1.249	0.686	0.294

Table 2. Classification matrix as obtained from LDA.

	Percent Correct	Apulia p=0.158	Latium p=0.184	Ligury p=0.132	Molise p=0.079	Sardinia p=0.105	Sicily p=0.105	Tuscany p=0.237
Apulia	50.00	3	2	1	0	0	0	0
Latium	57.14	1	4	0	0	1	0	1
Ligury	100.00	0	0	5	0	0	0	0
Molise	100.00	0	0	0	3	0	0	0
Sardinia	100.00	0	0	0	0	4	0	0
Sicily	100.00	0	0	0	0	0	4	0
Tuscany	88.00	1	0	0	0	0	0	8
Total	81.58	5	6	6	3	5	4	9

References

Angerosa, F., Bréas, O., Contento, S., Guillou, C., Reniero, F., & Sada, E. (1999). Application of stable isotope ratio analysis to the characterization of the geographical origin of olive oils. *Journal of Agriculture and Food Chemistry*, 47, 1013–1017.

Aparicio, R., & Aparicio-Ruı'z, R. (2000). Authentication of vegetable oils by chromatographic techniques. *Journal of Chromatography A*, 881, 93–104.

Baccouri, O., Guerfel, M., Baccouri, B., Cerretani, L., Bendini, A., Lercker, G., Zarrouk, M. Daoud Ben Miled, D. (2008). Chemical composition and oxidative stability of Tunisian monovarietal virgin olive oils with regard to fruit ripening. *Food Chemistry*, 109, 743–754.

Berezin, K. V., & Nechaev, V. V. (2005). Calculation of the IR Spectrum and the Molecular Structure of β-Carotene. *Journal of Applied Spectroscopy*, 72, 164-171.

Boschetti, T., & Iacumin, P. (2005). Continuous flow $\delta^{18}O$ measurements: new approach to standardization, high-temperature thermodynamic and sulphate analysis. *Rapid Communications in Mass Spectrometry,* 19, 1-8.

Camin, F., Larcher, R., Nicolini, G., Bontempo, L., Bertoldi, D., Perini, M., et al. (2010). Isotopic and elemental data for tracing the origin of European olive oils. *Food Chemistry*, 58, 570–577.

Casale, M., Casolino, C., Oliveri, P., & Forina, M. (2010). The potential of coupling information using three analytical techniques for identifying the geographical origin of Liguria extra virgin olive oil. *Food Chemistry*, 118, 163.

Chiavaro, E., Cerretani, L., Di Matteo, A., Barnaba, C., Bendini, A., & Iacumin, P. (2011). Application of a multidisciplinary approach for the evaluation of traceability of extra virgin olive oil. *European Journal of Lipid Science and Technology*, 113 (12), 1509–19.

Christopoulou, E., Lazaraki, M., Komaitis, M., & Kaselimis, K. (2004). Effectiveness of determinations of fatty acids and triglycerides for the detection of adulteration of olive oils with vegetable oils. *Food Chemistry*, 84, 463–474.

El-Abassy, R. M., Donfack, P., & Materny, A. (2009). Rapid determination of free fatty acid in extra virgin olive oil by Raman spectroscopy and multivariate analysis. *Journal of the American Oil Chemists' Society*, 86 (6), 507–511.

Gelder, J. D., Gussem, K. D., Vandenabeele, P., & Moens, L. (2007). Reference database of Raman spectra of biological molecules. *Journal of Raman Spectroscopy*, 38, 1133–1147.

Gimeno, E., Castellote, A.I., Lamuela, R., De la Torre, M.C., & Lopez-Sabater, M.C. (2002). The effects of the harvest and extraction methods on the antioxidant content (phenolics, alpha-tocopherol, and beta-carotene) in virgin olive oil. *Food Chemistry*, 78, 207–11.

Giuffrida, D., Salvo, F., Salvo, A., La Pera, L., & Dugo, G. (2007). Pigments composition in monovarietal virgin olive oils from various sicilian olive varieties. *Food Chemistry*, 101, 833–837.

Issaoui, M., Flamini, G., Brahmi, F., Dabbou, S., Ben Hassine, K., Taamali, A., Hechmi Chehabc, H., Ellouza, M., Zarroukd, M., & Hammamia, M. (2010). Effect of the growing area conditions on differentiation between Chemlali and Chétoui olive oils. *Food Chemistry*, 119, 220–225.

Korifi, R., Le Dreau, Y., Molinet, J., Artaud, J., & Dupuy, N. (2011). Composition and authentication of virgin olive oil from French PDO regions by chemometric treatment of Raman spectra. *Journal of Raman Spectroscopy*, 42 (7), 1540–1547.

Koyama, Y., Kito, M., Takii, T., Saiki, K., Kiyoshi, T., Sukida K., & Yamashita J. (1982). Configuration of the carotenoid in the reaction centers of photosynthetic bacteria. Comparison of the resonance raman spectrum of the reaction center of rhodopseudomonas sphaeroides g1c with those of cis-trans isomers of /i-carotene. *Biochimica et Biophvsica Acta*, 680, 109-118.

Longinelli, A., & Selmo, E., (2003). Isotopic composition of precipitation in Italy: a first overall map. *Journal of Hydrology*, 270, 75–88.

Mannina, L., Patumi, M., Proietti, N., Bassi, D., & Segre, A. L. (2001). Geographical characterization of Italian extra virgin olive oils using high-field H-1 NMR spectroscopy. *Journal of Agricultural and Food Chemistry*, 49, 2687–2696.

345 Merlin, J. C. (1985). Resonance Raman spectroscopy of carotenoids and carotenoid-containing
346 systems. *Pure and Applied Chemistry*, 57, 785–792.
347 Portarena, S., Farinelli, D., Lauteri, M., Famiani, F., Esti, M., & Brugnoli, E. (2015), Stable isotope
348 and fatty acid compositions of monovarietal olive oils: Implications of ripening stage and
349 climate effects as determinants in traceability studies. *Food Control*, 57, 129-135.
350 Portarena, S., Gavrichkova, O., Lauteri, M., & Brugnoli, E. (2014). Authentication and traceability
351 of Italian extra-virgin olive oils by means of stable isotopes techniques. *Food Chemistry*, 164,
352 12-16.
353 Rezzi, S., Axelson, D.E., Héberger, K., Reniero, F., Mariani, C., & Guillou, C. (2005). Classification
354 of olive oils using high throughput flow 1H NMR fingerprinting with principal component
355 analysis, linear discriminant analysis and probabilistic neural networks. *Analytica Chimica*
356 *Acta*, 552, 13–24.
357 Spangenberg, J.E., & Ogrinc, N. (2001). The application of NMR and MS methods for detection of
358 adulteration of wine, fruit juices, and olive oil. A review. *Journal of Agriculture and Food*
359 *Chemistry*, 49, 1534.
360 Tapp, H. S., Defernez, M., & Kemsley, E. K. (2003). FTIR Spectroscopy and multivariate analysis
361 can distinguish the geographic origin of extra virgin olive oils. *Journal of Agricultural and*
362 *Food Chemistry*, 51, 6110–6115.
363 Weng, Y.M., Weng, R.H., Tzeng, C.Y., & Chen, W. (2003). Structural analysis of triacylglycerols
364 and edible oils by near-infrared Fourier transform Raman spectroscopy. *Applied Spectroscopy*,
365 57, 413.
366 Woodcock, T., Downey, G., & O'Donnell, C. P. (2008). Confirmation of declared provenance of
367 European extra virgin olive oil samples by NIR spectroscopy. *Journal of Agricultural and Food*
368 *Chemistry*, 56, 11520–11525.

Yang, H., & Irudayaraj, J. (2001). Comparison of near-infrared, Fourier transform-infrared, and Fourier transform-Raman methods for determining olive pomace oil adulteration in extra virgin olive oil. *Journal of the American Oil Chemists Society*, 78, 889–895.

Young, K.E., Quinn, S.M., Trumble, S.J. (2012). Comparing Gas Chromatographic Techniques Used in Fatty Acid Profiling of Northern Fur Seals (Callorhinusursinus) and Steller Sea Lions (Eumetopiasjubatus) from Lovushki Island Complex, Russia. *International Journal of Applied Science and Technology*, 9, 11-21.

Zou, M.-Q., Zhang, X.-F., Qi, X.-H., Ma, H.-L., Dong, Y., Liu, C.-W., Guo, X., & Wang, H. (2009). Rapid authentication of olive oil adulteration by Raman spectrometry. *Journal Agricultural of Food Chemistry*, 57, 6001–6006.

Figure 1

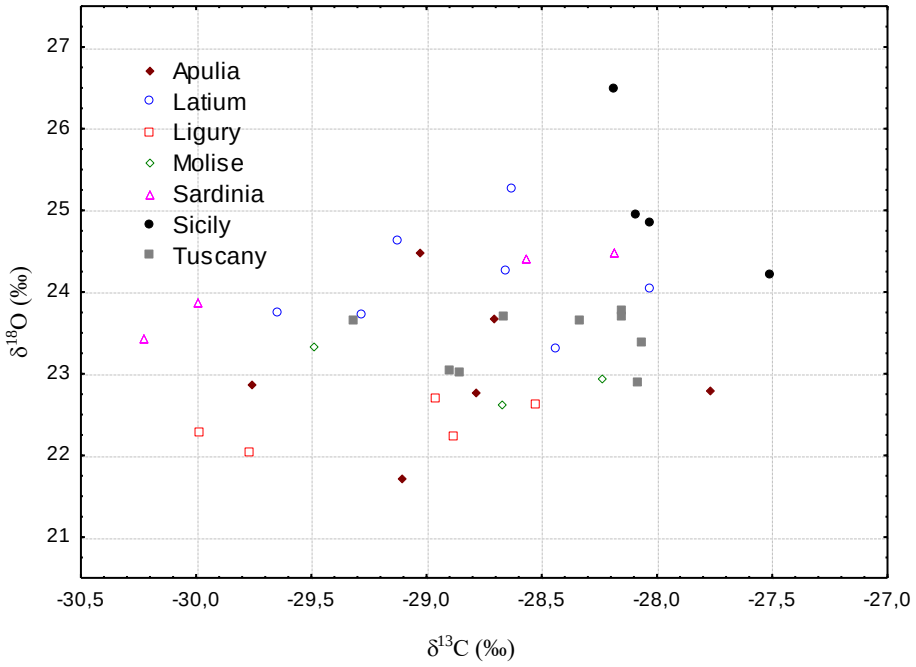
Apulia
Latium
Ligury
Molise
Sardinia
Sicily
Tuscany
27
26
25
24
23
22
21
δ18O (‰)
-30,5
-30,0
-29,5
-29,0
-28,5
-28,0
-27,5
-27,0
δ13C (‰)

Figure 2

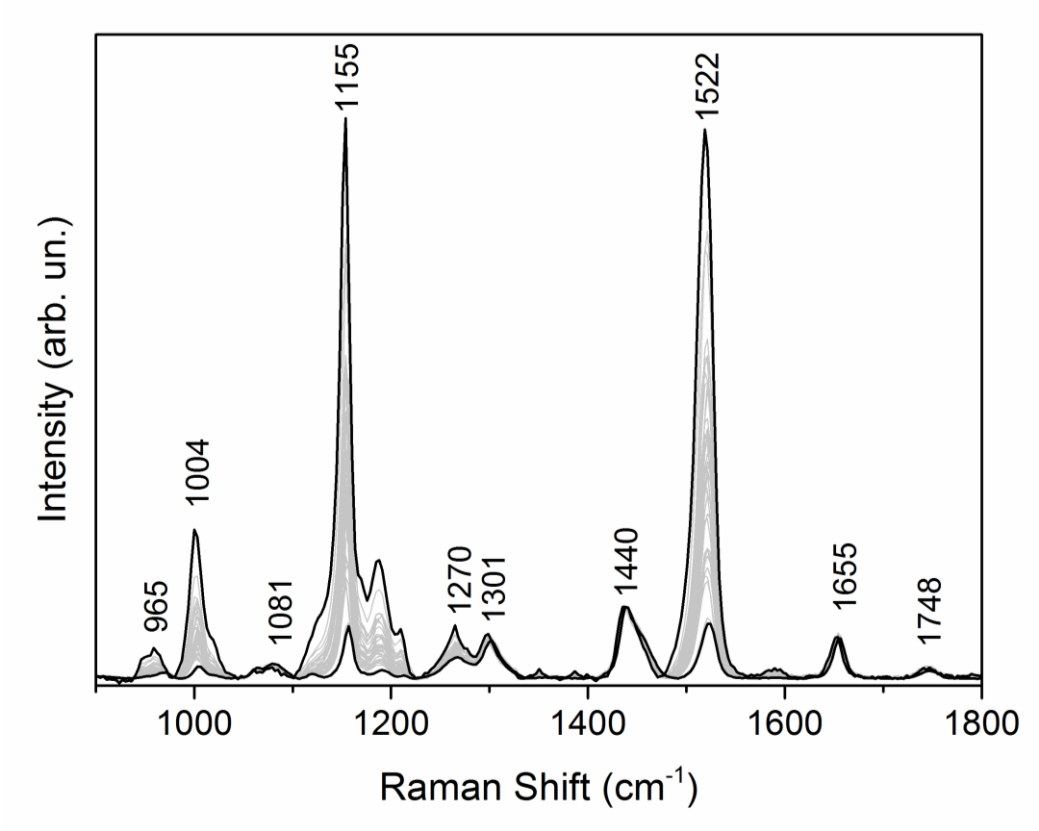
Intensity (arb. un.)
965
1004
1081
1155
1270
1301
1440
1522
1655
1748
1000
1200
1400
1600
1800
Raman Shift (cm-1)

Figure 3

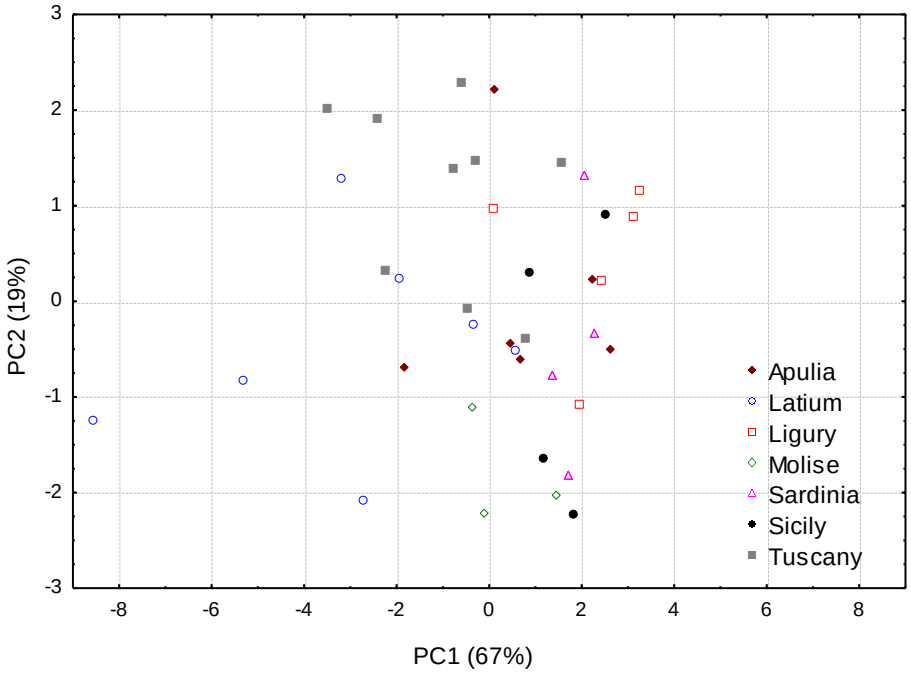
PC2 (19%)
PC1 (67%)
3
2
1
0
-1
-2
-3
-8
-6
-4
-2
0
2
4
6
8
Apulia
Latium
Ligury
Molise
Sardinia
Sicily
Tuscany

Figure 4

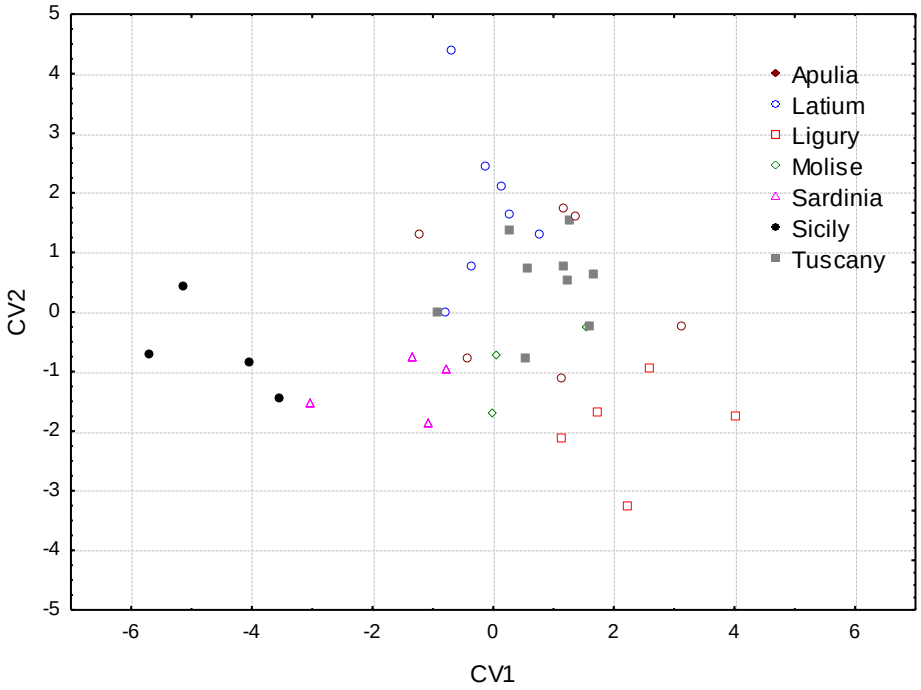
5
4
3
2
1
0
-1
-2
-3
-4
-5
CV2
-6
-4
-2
0
2
4
6
CV1
Apulia
Latium
Ligury
Molise
Sardinia
Sicily
Tuscany